Characterising the reliability of production from future British offshore wind fleets

CHARACTERISING THE RELIABILITY OF PRODUCTION FROM FUTURE BRITISH OFFSHORE WIND FLEETS

S. Hawkins, D. Eager, G.P. Harrison*

*Institute for Energy Systems, School of Engineering, University of Edinburgh; *Gareth.Harrison@ed.ac.uk*

Keywords: Capacity value, offshore wind generation, mesoscale modelling.

Abstract

The extent to which large volumes of offshore wind can contribute to a secure and reliable electricity supply is a subject of much debate. Key to providing credible answers requires a detailed understanding of the wind resource and its variability in time and space. Here, a mesoscale atmospheric model was employed to create a ten year hindcast of British onshore and offshore wind speeds. This was used to simulate the output of a British offshore wind fleet and combined with demand data to assess reliability during periods of high demand. Further, capacity value calculations using Effective Load Carrying Capability for the combined onshore and offshore GB wind fleet provides an estimate of the long-term reliability of production.

1 Introduction

Integrating large amounts of variable renewable generation into the electricity network presents a significant challenge and is the subject of much debate. This is particularly true in the UK where wind generation is expected to become a significant supplier of energy, with a large increases in capacity expected offshore, perhaps in excess of 30GW by 2030, up from around 1GW today.

Debate centres on the question: 'to what extent can a variable and stochastic resource contribute to a secure and reliable electricity supply?' Key to answering this is a detailed understanding of the wind resource and its variability in time and space. However, there are relatively few sources of offshore observations with sufficient temporal resolution or accuracy to address this. In a future system with high penetrations of wind, the temporal variability of wind will determine numerous characteristics such as the capacity value of wind and the amount of reserve required to maintain an adequate level of system security.

This paper presents the results of a high resolution re-analysis using a mesoscale atmospheric model to recreate ten years of hourly wind speeds across Great Britain (GB) and surrounding waters. Wind speeds are extensively validated against observations from a number of available buoys, lightships and offshore platforms. The dataset is used to simulate ten years of wind production. Taking inspiration from capacity value calculations for onshore wind [1] this new data is used to produce the first credible estimate of the contribution of British offshore wind generation in supporting demand.

2 Mesoscale modelling

2.1 Simulation

Mesoscale atmospheric modelling is becoming widely used in the wind energy field, both for short-term forecasting and longer-term resource assessment. Mesoscale models are computationally demanding, so many studies either simulate relatively short time periods or employ statistical downscaling to reduce the computational requirement needed to capture a representative period. However, short term analyses do not fully capture wind speed variability, while statistical approaches do not produce continuous historic time-series which can be matched with historic patterns of energy demand.

This study uses the Weather Research and Forecast (WRF) model [7], a fully-compressible non-hydrostatic mesoscale model with multiple boundary-layer, land surface, microphysics and cloud physics options. The model was configured with three nested domains down to 3km resolution (Figure 1). Boundary conditions were taken every six hours from the NCEP Global Forecast System Final Analysis dataset at 1^{o} resolution. Two- way nesting and analysis nudging was used on all domains. The main physics options are summarised in Table 1.

Ten years were simulated, from 2001-2010 inclusive, on the UK Research Council's high performance computing platform, HECToR.

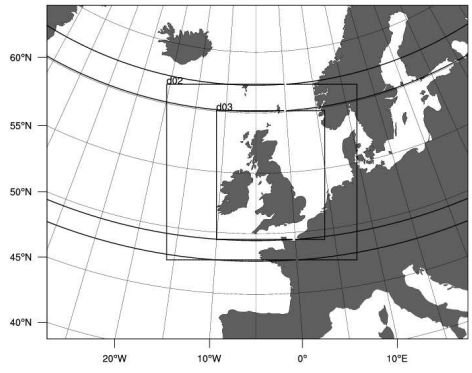

Figure 1: Nested domains at 27, 9 and 3km resolution

Domain	1	2	3
Resolution (km)	27	9	3
Integration timestep (s)	135	45	15
Analysis nudging	y	y	y
Cumulus scheme	Kain-Fritsch		None
PBL scheme	MYJ [4]		
Surface layer	Monin-Obhukhov [5]		
Land surface scheme	NOAH		
Land use dataset	MODIS		

Table 1. Summary of mesoscale model configuration.

WRF uses a terrain-following, pressure based vertical coordinate system. The vertical resolution was increased close to the ground to reduce any errors associated with interpolation to fixed heights. Wind speeds were interpolated to hub height from the closest model level:

$$U_z = U_m \cdot \ln(z / z_0) / \ln(z_m / z_0) \quad (1)$$

where U_z is the wind speed at hub height z. U_m is wind speed at the closest model level z_m and z_0 is the local roughness length taken from WRF. Over water, WRF uses a Charnock formulation for roughness length.

2.2 Wind farm load factor

For existing (as well as planned and under construction) onshore and offshore wind farms, hourly wind speeds were converted to power output using the manufacturer's power curve for the appropriate turbine. The make, model and size of turbine are specified in the RenewableUK wind farm database.

The location of future offshore wind farms were taken from the Crown Estate leasing rounds. A generic 3MW turbine was assumed for Round 2 sites, and a generic 5MW turbine for Round 3, based on commercially available models. The final installed capacity in each offshore site was assumed to be distributed in proportion to the maximum lease capacities.

Overall GB-level aggregate load factors (LFs) were computed as averages weighted by final installed capacity. That is, if LF_i^n represents the LF of wind farm n at time t, then the aggregate LF at time t is calculated as:

$$LF_t = \sum_{n=1}^{N} (LF_t^n \cdot C^n) / \sum_{n=1}^{N} C^n \quad (2)$$

where C^n is the final installed capacity of wind farm n. Aggregate offshore and onshore LF are calculated separately, i.e. n is restricted to either offshore or onshore farms. For offshore farms, this means longer term calculations are weighted towards the larger Round 3 sites.

2.3 Validation

Wind speeds were validated against onshore met stations and offshore buoys, lightships and platforms. Standard error statistics of Bias (B), Mean Percentage Error (MPE), Root-Mean-Square Difference (RMSD) and coefficient of determination (R^2) were calculated.

	n	B	MPE	RMSD	R^2
		m/s	%	m/s	
Met stations	220	0.02	-0.5	0.44	0.96
Buoys	9	0.24	6.25	1.16	0.82
Lightships	4	-0.38	-1.99	1.30	0.91
Platforms	3	0.30	3.48	1.54	0.93

Table 2. Summary of error statistics by observation type

Table 2 summarises the error statistics by class of observation. The performance is generally good, with high correlation values. Onshore the agreement between simulated and observed wind speeds was very good, with overall high correlation and low bias. Offshore a seasonal bias of -1 to -2ms was found in summer months. This merits further investigation, however it does not affect the capacity value analysis presented here which is based only on winter wind speeds.

Monthly measured LFs for the largest onshore wind farms in each region of the UK (covering 196 wind farms with a totalled installed capacity of 2.7GW) were compiled from Ofgem's Renewable Obligation Certificate (ROC) Register for the period from April 2006 to December 2010. LFs for existing offshore wind farms were also compiled from the time they became operational until December 2010. By the end of that period, that amounted to 8 wind farms with a total installed capacity of around 1 GW.

Simulated LFs at the same sites were derived from the modelled hourly wind speeds and then averaged to monthly values. No accounting for wake losses or other array losses was carried out at this stage. Figures 2 and 3 show the agreement between average monthly LF averaged across onshore and offshore sites. Onshore, the predicted LFs were found to be consistently higher than observed. This would be expected before losses have been considered. A linear scaling factor of 0.69 gave the best adjustment between simulated and observed LFs (R^2=0.94).

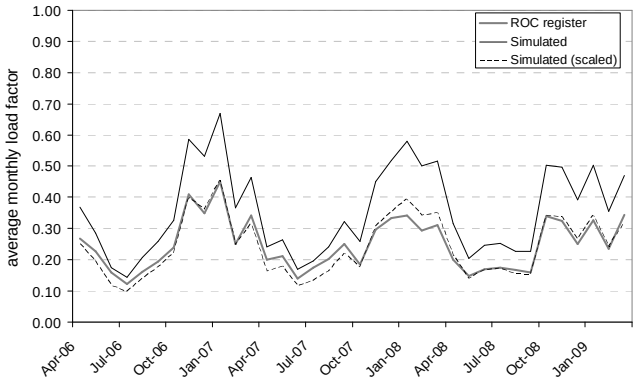

Figure 2: Average monthly LF for existing onshore wind farms. The thick grey line shows the actual weighted average LF from 196 large wind farms. The solid black line shows simulated LFs at 100% availability/no losses and the dashed line shows these values scaled by 0.69.

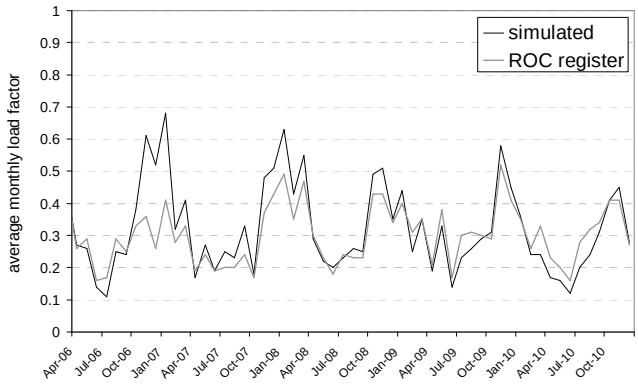

Figure 3: Average monthly LFs for existing offshore wind farms. The thick grey line shows weighted average LF for all operational offshore The solid black line shows simulated LFs with no adjustment for losses. The large deviation in the first winter period is due to low technical availability in the early stages of some offshore farms.

Offshore, the predicted LFs were already in quite close agreement to the observed values, except for two winter periods were technical availability at a number of offshore wind farms was very low. LFs were slightly too low in summer, confirming the seasonal wind speed bias seen at observation sites. For this reason, no further accounting for wake losses or technical availability was performed for offshore sites.

3 Reliability analysis

3.1 Historic wind and demand time series

The relationship between wind generation and electrical demand is of primary interest when analysing the reliability of the wind resource. Of particular interest is the availability of the wind resource during periods of high demand. In Britain the highest demands are driven by low temperatures occurring during winter (November-March). It is during these periods that the adequacy risk is typically highest.

Historic aggregated half-hourly demand data going back to April 2001 is available from the GB System Operator (SO), National Grid [9]. The GB 'IO14_DEM' data is the most applicable for generation adequacy calculations because this is based on operational generation metering and includes station load and pumped storage (PS) pumping [1]. However this data is inconsistent as prior to April 2005 it relates to England and Wales only. The 'INDO' demand measure, which excludes station load and PS pumping, is available for the entire period. The winter 'IO14_DEM' values can be approximated by raising the 'INDO' measure by 600 MW and is used where the 'IO14_DEM' data is not available.

To account for underlying changes in absolute levels of peak demand, each winter's demand is normalised by out-turn "Average Cold Spell" (ACS) peak demand and rescaled to 60 GW. ACS peak demand is forecast each year in advance of the forthcoming winter by the SO, and is described as having "a 50% chance of being exceeded as a result of weather variation alone" [8]. The out-turn ACS peak is calculated post winter and is a measure of what peak demand would be given a winter's underlying demand patterns and "typical" winter peak weather conditions [8]. This makes it suitable value for the normalisation. These values can be found in [1] and [10].

The half-hourly data is transformed to hourly resolution by taking the hourly demand to be the maximum of the two half-hour periods. Finally, the normalised hourly demand data is then matched with the hourly simulated wind LFs. The time series spans 9.5 consecutive winters from winter 2001/02 to December 2010, totalling 34,128 demand hours.

Figure 4 shows the simulated average aggregate long-term LFs for wind generation during the highest demand hours. The 90%+ normalised demand hours are categorised into 1% bins and the cumulative number of hours at each demand level are indicated on the graph (i.e., each label indicates the number of hours demand is at or above *x*). Note that demand levels above 100% of peak are possible on account of ACS peak being exceeded in some years. Interestingly, the pattern of average LFs shows a good agreement with the analyses of transmission metered wind farms presented in [14]. However absolute levels of average LF are higher with around a 45% LF at 90% to 95% levels of demand compared to 20% in [14]. This is hardly surprising given the increased geographic diversity of the wind capacity. As mentioned earlier, no scaling factors were applied to the simulated offshore LFs, which may lead to systematic over-estimation in the results. Therefore a second case where weighted offshore LFs are scaled by 0.69 is also included in Figure 4. This reduces the average LF at 90% to 95% demand levels to around 35%. The level of deterioration in average LFs at high demands is less severe than in [14], although this is based on just 2 hours of simulated data. It highlights the challenge for determining the availability of wind at high demand levels [14].

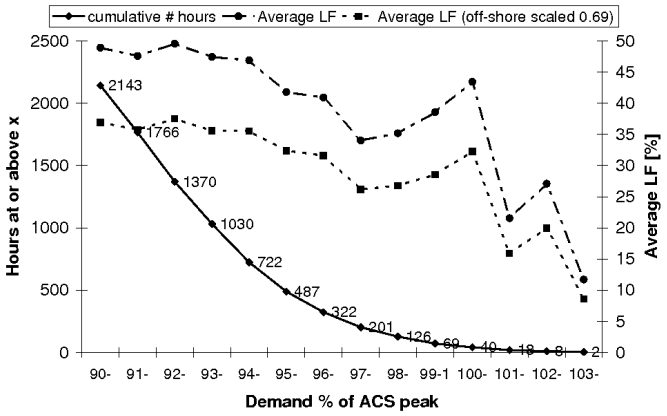

Figure 4. Average long-term LFs for highest demand levels (right y-axis): base-case and wind scaled by 0.69 (upper and lower dashed lines). The demand hours per 1% normalised demand bin are shown on the left y-axis.

3.2 Risk metrics

The loss-of-load probability (LOLP) in a particular period is defined as the probability that available generation is unable to meet demand:

$$LOLP = p(X < D), \quad (3)$$

where X is the available generation and D is the system demand, both of which are random variables. The loss-of-load expectation (LOLE) is the expected number of periods over a given period in which available generation is unable to meet demand. So for a given time horizon:

$$LOLE = \sum_{t}^{T} LOLP_t, \quad (4)$$

where $LOLP_t$ is the LOLP in period t. Here, the period t is assumed to be one hour and T spans a number of years.

3.3 Capacity value calculations

The use of capacity value is common when measuring the contribution of renewable energy generation to meeting demand. Here the Effective Load Carrying Capability (ELCC) defines the capacity value (or capacity credit). The ELCC for a particular level of additional generating capacity estimates the amount of additional demand that can be served due to the extra generation whilst maintaining the original level of system risk [6]. The purpose of this study is to demonstrate an application of the mesoscale model, not to determine an absolute measure of wind generation capacity value for GB. Moreover, a specific methodology has been applied to calculate capacity value, and while the authors concede that this is not necessarily cutting edge probability theory (e.g., see [14]) it is a fully valid contribution to defining current approximations of capacity value in GB (e.g., [11,12]). What is more, this is understood to be the first time that capacity value for a combined on- and offshore wind resource has been calculated using the ELCC approach.

The capacity value is estimated as follows. Consider some additional wind generation w which increases overall system capacity. If the system LOLP in hour t before the additional generation is added is the "initial" LOLP, then adding the additional generation will reduce the LOLP. The total reduction depends on the reliability of the additional generation. This reduced LOLP can be expressed by:

$$LOLP^* = p(X < D - W), \quad (5)$$

where W is the contribution to demand from the additional generation. Similarly, using the same principle as (4), the reduced 9.5 winter LOLE can also be determined.

The ELCC for the additional generation is found by increasing demand until the reduced LOLP* risk returns to its original value. Here the interest is in the ELCC across the entire time horizon; however calculation of the ELCC for a single period is the starting point. This is given by [14]:

$$p(X < D) = p(X < D + d_{ELCC} - W), \quad (6)$$

where d_{ELCC} is the ELCC. This can be extended over multiple periods to:

$$\sum_{t}^{T} p(X_t < D_t) = \sum_{t}^{T} p(X_t < D_t + s_t d_{ELCC} - W_t), \quad (7)$$

where s_t is a scalar applied to the ELCC in order to account for the level of demand being experienced. Or put another way, the scalar places a higher weight on the highest demand periods when solving (7).

3.3.1 Treatment of conventional generation

The next step is to construct a probability distribution for available conventional generation. Here, the term conventional generation covers all forms of generation currently connected to the high voltage transmission system in GB, with the exception of wind. Furthermore, the availability of conventional generation is assumed to be independent of demand and available wind capacity. Technical plant availability data is not available in GB. However most generating companies try to make available as much capacity as possible at time of highest demand (to not forgo high wholesale market prices), thus availability is a function of the unit's forced outage rate (FOR), which it is reasonable to assume are independent [1].

Generation unit data is taken from the National Grid Seven Year Statement [10] and the expected winter peak availabilities in their Winter Outlook [11] are used as FORs. This data is summarised in Table 3. The Unit Effective Capacity (UEC) in [10] has been used for all units, apart from those which are transmission constrained; in this case the individual UEC is scaled in order to match the transmission limit. Hydro units belonging to the same hydro scheme are combined into single pseudo-units owing to their resource interdependence.

Power station type	*No. units*	*Capacity (GW)*	*Assumed availability*
Nuclear	22	10.1	0.75
Interconnector	1	2	1.00
Hydro	9	1.1	0.60
Coal	62	27.9	0.90
Oil	4	2.7	0.80
Pumped storage	16	2.7	1.00
OCGT	34	1.2	0.90
CCGT	124	26.7	0.90
TOTAL	272	74.4	

Table 3: Transmission connected conventional unit types [11].

The capacity outage probability table technique [2] assumes available capacity follows a Bernoulli distribution between zero and full capacity. With a 1 MW bin size, the resulting aggregate probability density functions have mean and standard deviation of 65.3 GW and 1.8 GW, respectively. Using this distribution the hourly winter LOLPs can be computed (3).

For simplicity each normalised hourly *d* is assumed to be fixed and does not itself follow an assumed probability distribution. Hourly LOLPs can be summed to produce the total 9.5-winter LOLE (4). Similarly the reduced LOLE is calculated using the expected wind output at each hour estimated by the numerator of (2).

3.3.2 Build-based capacity value: focus on offshore wind

Initially the offshore wind resource is considered in isolation with particular interest in the relationship between the spatial distribution of generation capacity and capacity value. The hourly aggregated GB offshore wind LFs are estimated using a projected offshore wind build schedule. This timetable is constructed from the three Crown Estate auctions (rounds 1-3) that define the locations and expected capacities of the offshore farms (see [13]). The aggregate LFs are then derived using the geographically weighted average of locational LFs (2). The results of this analysis are illustrated in Figure 5.

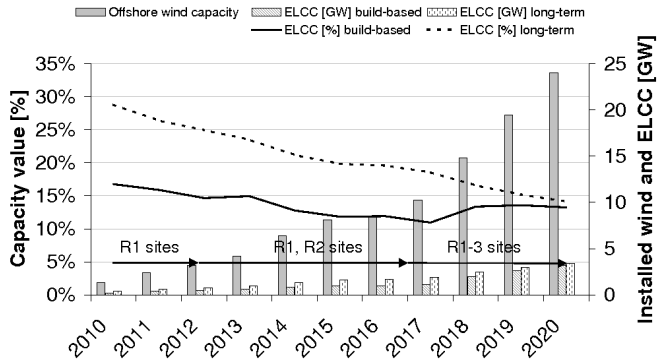

Figure 5. Capacity value (left y-axis) and ELCC (right y-axis) results for GB offshore wind using long-term and build-based LFs.

The dashed line shows capacity values calculated using *long-term* aggregate weighted LFs. This assumes all sites are included and the contribution from individual locations scaled by weighting their capacities. The solid line shows the capacity values calculated using the *build-based* aggregate weighted LFs over just the wind farm sites expected to be online at the start of each year considered. The total installed capacity expected to be online by the stated year is the same in both cases, however the build-based LFs are weighted across a less diverse resource. The graph demonstrates that considering sites by build schedule leads to lower estimated capacity values with the monotonically decreasing characteristic common in capacity value plots not present (e.g., Figure 7). This can be explained by the added value of capacity diversity improving (but not eliminating) the impact of dependence between sites on resource reliability in some years (particularly for the larger Round 3 sites).

Further, the box in Figure 6 shows the expected availability and standard deviation of offshore wind capacity during high demand hours (note that the total installed capacities are as in Figure 5). In this case, those demand hours within 5% of peak provide a sample size of 655 hours over the 9.5 winters. The selected probability mass functions demonstrate how the distribution of aggregate LFs for the sampled hours changes over time. There is a visible reduction in expected low LF hours as geographical diversity increases, and the probability of high loads factors remains high relative to those typically simulated for onshore (e.g., [1]).

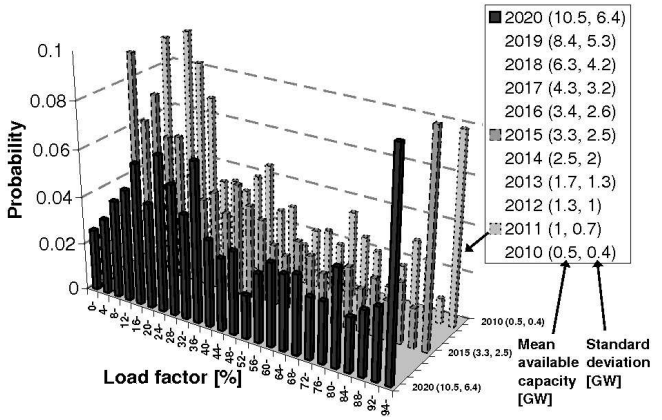

Figure 6. Probability mass function for GB off-shore wind LFs for selected years based on demand hours within 5% of annual peak. If the LF falls in a particular range (x-axis), it is deemed to be at the middle of that range (i.e., LFs in the range 0-4% are deemed to be 2%). Mean and standard deviation of total available capacity depicted in box.

3.3.3 Aggregate GB wind capacity value

Attention now turns to the combined GB wind resource, Figure 7 shows the ELCC and corresponding capacity value results for combined on- and offshore analysis using the long-term aggregate weighted LFs. These results suggest that for high levels of highly geographically diverse installed capacity, a capacity value of 10% appears credible.

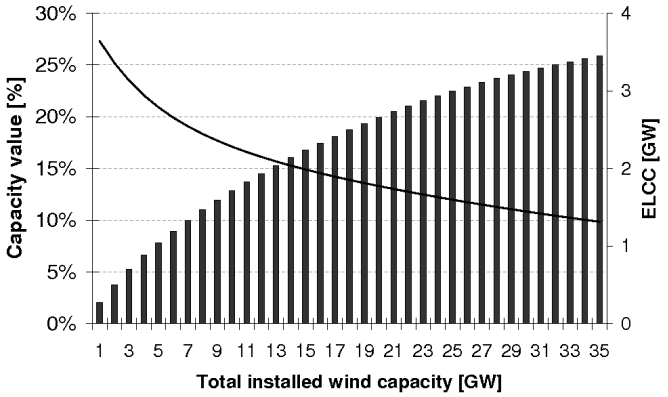

Figure 7. Capacity value (left y-axis, line) and ELCC (right y-axis, bars) for the combined on and offshore GB wind resource calculated with long-term aggregate LFs.

Figure 8 shows the results of a sensitivity analysis for ELCC that included the following (the numbers match Figure 8):

1) Scaling factor 0.69 applied to long-term offshore weighted loads factors;

2) Normalised peak demand reduced from 60 to 57 GW (initial LOLE reduced by 99%);
3) Reducing the total available conventional generation by 4 GW to a distribution with mean 62.2 GW, and standard deviation 1.7 GW (initial LOLE increases by 3000%).

As might be expected with sensitivity factor 1 the effect of scaling offshore wind LFs downwards tends to reduce the capacity value of wind. In 2 the risk is reduced, so is the ELCC and capacity value is also reduced. In 3 the risk increases and the ELCC does likewise. This is a well-known result of ELCC analysis and demonstrates the impact of underlying system risk on the results obtained.

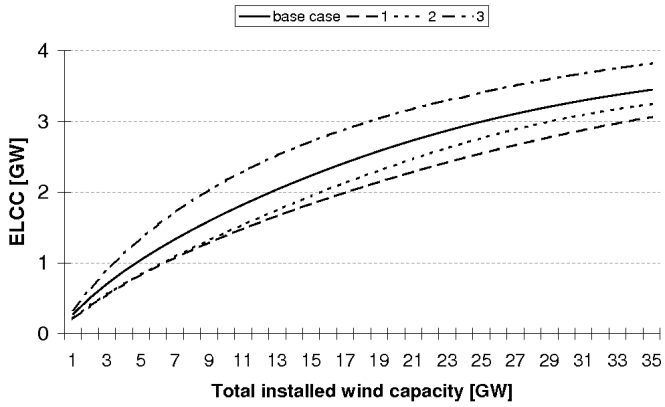

Figure 8. Sensitivity of ELCC value to assumptions.

4 Discussion

A major assumption here is that the last ten years winds are reasonably representative of future wind in the UK. Ten years is not enough to represent a full climatology and there is evidence of climate change affecting wind speeds [3]. However, ten years is long enough to sample a wide range of synoptic conditions and weather types and the analysis is a substantial improvement on comparable studies.

The output of wind at times of peak demand varies considerably between years. For example, in 2010, blocking high pressure over northern Europe led to very cold temperatures and high electrical demand, yet low wind speeds persisted over the UK. This highlights the difficulty, perhaps even the validity, of attempting to represent the contribution wind makes towards reliability as a single figure.

5 Conclusion

A detailed understanding of the wind resource and its variability in time and space is vital for understanding the contribution of offshore wind to reliable electricity supply. Here, a mesoscale atmospheric model was employed to create an ten year hindcast of British offshore wind speeds and simulated production.

Results of a reliability analysis have provided insight into the reliability of production from offshore wind at periods of high demand. What's more, credible estimates of combined long-term onshore and offshore capacity value have been derived and the sensitivities of these estimates to the underlying level of system risk discussed.

Acknowledgements

The authors acknowledge valuable input from Dr Chris Dent of Durham University. The PhD studentships awarded to S. Hawkins by the EPSRC Supergen Flexnet consortium and Kier Watson Trust and to D. Eager by the UK Energy Research Centre are gratefully acknowledged.

References

[1] P. Aguirre, C. Dent, G. Harrison, and J. Bialek, "Realistic Calculation of Wind Generation Capacity Credits," *CIGRE/IEEE PES Joint Symposium on Integration of Wide-Scale Renewable Resources Into the Power Delivery System*, July 2009.

[2] R. Billinton and R. N. Allan, *Reliability Evaluation of Power Systems. 2nd ed.* Plenum, 1994.

[3] G. P. Harrison, L. C. Cradden and J. P. Chick, "Preliminary assessment of climate change impacts on the UK onshore wind energy resource", *Energy Sources*, 30 (14), 1286-1299. 2008.

[4] Z. I. Janjic, "Nonsingular implementation of the Mellor-Yamanda level 2.5 scheme in the NCEP global model." *National Center for Environmental Prediction* Office Note, no 437. 2002

[5] Z. I. Janjic, "The surface layer in the NCEP Eta Model." In A. M. Soc (Ed.), *Eleventh Conference on Numerical Weather Prediction* (pp. 354-355). Norfolk, VA. 1996.

[6] A. Keane, M. Milligan, C. J. Dent, B. Hasche, C. D'Annunzio, K. Dragoon, H. Holttinen, N. Samaan, L. Soder, and M. O'Malley, "Capacity Value of Wind Power," *IEEE Transactions on Power Systems*, 26 (2), 2010, 564 – 572.

[7] J. B. Klemp, D. O. Gill, D. M. Barker, M.G. Duda, W. Wang, J. G. Powers, "A Description of the Advanced Research WRF Version 3". *National Center for Atmospheric Research*. Technical Note 2008.

[8] National Grid, "Average Cold Spell (ACS) Correction." nationalgrid.com/uk/sys_08/default.asp?action=mnch2_15.htm&sNode=2&Exp=N.

[9] National Grid, "Operational Data." nationalgrid.com/uk/Electricity/Data/Demand+Data/.

[10] National Grid, "Seven Year Statements," www.nationalgrid.com/uk/Electricity/SYS/.

[11] National Grid, "Winter Outlook Consultation 2010/11," www.nationalgrid.com/uk/Gas/TYS/outlook/.

[12] N. Screen, V. Parail, D. Sinclair, and O. Rix, "Electricity Market Reform Analysis of Policy Options," Redpoint Energy, Dec. 2010. www.decc.gov.uk/en/content/cms/consultations/emr/emr.aspx

[13] RenewableUK, formerly the British Wind Energy Association. www.bwea.com.

[14] S. Zachary and C.J. Dent, "Probability theory of capacity value of additional generation" www.supergen-networks.org.uk/filebyid/609/file.pdf. 2011